



Deposited via The University of Leeds.

White Rose Research Online URL for this paper:

<https://eprints.whiterose.ac.uk/id/eprint/161039/>

Version: Accepted Version

Article:

Thomas, SA, Mishra, B and Myneni, SCB (2020) Cellular Mercury Coordination Environment, and Not Cell Surface Ligands, Influence Bacterial Methylmercury Production. *Environmental Science & Technology*, 54 (7). pp. 3960-3968. ISSN: 0013-936X

<https://doi.org/10.1021/acs.est.9b05915>

© 2020 American Chemical Society. This is an author produced version of a paper published in *Environmental Science & Technology*. Uploaded in accordance with the publisher's self-archiving policy.

Reuse

Items deposited in White Rose Research Online are protected by copyright, with all rights reserved unless indicated otherwise. They may be downloaded and/or printed for private study, or other acts as permitted by national copyright laws. The publisher or other rights holders may allow further reproduction and re-use of the full text version. This is indicated by the licence information on the White Rose Research Online record for the item.

Takedown

If you consider content in White Rose Research Online to be in breach of UK law, please notify us by emailing eprints@whiterose.ac.uk including the URL of the record and the reason for the withdrawal request.

Cellular mercury coordination environment, and not cell surface ligands, influence
bacterial methylmercury production

Sara A. Thomas,*¹ Bhoopesh Mishra,² and Satish C. B. Myneni¹

¹ Department of Geosciences, Princeton University, Guyot Hall, Princeton, NJ, 08544

² School of Chemical and Process Engineering, University of Leeds, Leeds LS2 9JT, UK

* Corresponding author:

Sara A. Thomas

Email: st18@princeton.edu

Phone: (609)-258-2339

1 **Abstract**

2 Conversion of inorganic mercury (Hg(II)) to methylmercury (MeHg) is central to the
3 understanding of Hg toxicity in the environment. Hg methylation occurs in the cytosol of certain
4 obligate anaerobic bacteria and archaea possessing the *hgcAB* gene cluster. However, the processes
5 involved in Hg(II) biouptake and methylation are not well understood. Here we examined the role
6 of cell surface thiols, cellular ligands with the highest affinity for Hg(II) that are located at the
7 interface between the outer membrane and external medium, on the sorption and methylation of
8 Hg(II) by *Geobacter sulfurreducens*. The effect of added cysteine (Cys), which is known to greatly
9 enhance Hg(II) biouptake and methylation, was also explored. By quantitatively blocking surface
10 thiols with a thiol binding ligand (qBBR), we show that surface thiols have no significant effect on
11 Hg(II) methylation, regardless of Cys addition. The results also identify a significant amount of
12 cell-associated Hg-S₃/S₄ species, as studied by high energy-resolution X-ray absorption near edge
13 structure (HR-XANES) spectroscopy, under conditions of high MeHg production (with Cys
14 addition). In contrast, Hg-S₂ are the predominant species during low MeHg production. Hg-S₃/S₄
15 species may be related to enhanced Hg(II) biouptake or the ability of Hg(II) to become methylated
16 by HgcAB and should be further explored in this context.

17

18

19

20

21

22

23

24 **Introduction**

25 Mercury (Hg) is a global pollutant that is highly bioaccumulative and neurotoxic in its chief
26 environmental organic form (i.e., methylmercury – MeHg or CH₃Hg⁺). Certain obligative
27 anaerobic bacteria and archaea are the primary source of MeHg,¹⁻³ which is produced from
28 inorganic Hg(II) in the cell cytosol.⁴ Thus, understanding the biogeochemical factors that lead to
29 the microbial biouptake and subsequent methylation of Hg(II) is crucial to develop models for
30 determining the potential for MeHg production in the environment.

31 Chemical Hg(II) speciation is a critical factor that controls whether Hg(II) biouptake and
32 methylation can occur in the environment. Hg(II) has a high affinity for reduced sulfur (i.e., thiols
33 and sulfides), and the formation constants of Hg(II)-thiol and inorganic Hg(II)-sulfide species can
34 be at least 20 orders of magnitude greater than those of Hg(II) complexes with carboxyls, amines,
35 and most inorganic ligands.^{5, 6} Thus in natural environments, Hg(II) is expected to be bound to
36 thiols (e.g., natural organic matter and low molecular weight – LMW – organic ligands) and/or
37 inorganic sulfides (e.g., particulate and dissolved mono- and polysulfides) under sulfidic
38 conditions.⁷

39 While much attention has been given to understanding the biouptake of Hg(II)-thiol and
40 Hg(II)-sulfide species by Hg-methylating organisms, the mechanisms and pathway(s) of Hg(II)
41 biouptake are not well understood. Most studies rely on thermodynamic stability constants to
42 obtain chemical Hg(II) speciation information for Hg(II) uptake and methylation assays.⁸⁻¹⁵ This
43 methodology has led to current Hg(II) biouptake paradigms, which include the passive uptake of
44 neutral Hg(II)-sulfide complexes (e.g., HgS⁰ or Hg(HS)₂⁰)⁸⁻¹¹ and the active uptake of Hg(II)
45 complexes with LMW thiols (e.g., Hg(cysteine)₂).^{12, 13} However, microbes can alter extracellular
46 Hg(II) speciation by the degradation or secretion of Hg(II)-binding ligands (e.g., sulfide and

47 cysteine)¹⁶⁻²⁰ as well as cell-associated Hg(II) speciation via reactions with cellular S-containing
48 ligands.^{16-18, 21-24} Therefore, predictions for Hg(II) speciation based on the initial composition of
49 the exposure medium are not always accurate throughout the duration of the assay. In contrast,
50 directly tracking the cell-associated Hg(II) coordination environment during Hg exposure assays
51 can provide insight into the Hg(II) uptake and methylation mechanisms. Yet, only a few studies
52 have captured Hg(II) coordination information during microbial Hg uptake^{16-18, 22, 25} and even
53 fewer have studied Hg(II) coordination in organisms actively methylating Hg^{17, 25} due to the
54 inherently low concentrations of cell-associated Hg. Furthermore, the Hg coordination
55 environment in Hg-methylating organisms at environmentally-relevant Hg concentrations has yet
56 to be explored.

57 The recent developments in high energy-resolution X-ray absorption near edge structure
58 (HR-XANES) spectroscopy now makes the assessment of Hg(II) coordination in dilute systems
59 (sub-ppm Hg) possible,^{16, 26-30} specifically at the ambient Hg to cell ratios at which environmental
60 Hg methylation is of concern. Herein, we employ Hg L₃-edge HR-XANES spectroscopy to directly
61 monitor the coordination chemistry of Hg in actively Hg-methylating cells. Specifically, we
62 explore the effect of extracellular cysteine (Cys) addition as well as the role of cell surface thiols
63 on the sorption, methylation, and Hg(II) coordination by the model Hg-methylating bacterium
64 *Geobacter sulfurreducens*. Cell surface thiols make up roughly 5 – 10% of the total surface
65 functional groups,³¹ can form complexes with Hg,^{21-24, 31, 32} and may even adsorb or act as a
66 nucleation site for HgS_(s) nanoparticles.¹⁷ Metal sorption to cell surface functional groups is a
67 primary step in general metal biouptake models,³³ and Hg(II) sorption to surface thiols has recently
68 been proposed to control Hg(II) uptake and methylation under environmental conditions.²⁰ Yet,
69 the role of cell surface thiols in MeHg production has not been directly explored. Because

70 exogenous cysteine (Cys) is known to greatly enhance Hg(II) uptake and methylation by *G.*
71 *sulfurreducens*,¹⁴ we compare our results in the presence and absence of added Cys.

72 **Materials and Methods**

73 ***Bacterial strain and growth medium.*** *Geobacter sulfurreducens* PCA was gratefully obtained
74 from Dr. Jeffra Schaefer, Rutgers University. *G. sulfurreducens* was grown statically at 29 °C in a
75 dark water bath in defined medium from Schaefer et al.¹⁴ containing (g per L): MOPS buffer (2.1),
76 NH₄Cl (0.005), NaH₂PO₄ (0.006), sodium acetate (0.82), sodium fumarate (6.4), resazurin (0.001),
77 and trace metals (10 mL per L; Table S1) at pH 6.8 (adjusted with NaOH). The growth and assay
78 media were made anoxic by boiling and cooling while bubbling with N₂ gas. Hungate tubes and
79 acid-washed serum bottles containing the anoxic media were crimp sealed with rubber septa and
80 autoclaved. Once exponential growth phase was reached (OD₆₀₀ = 0.1 – 0.2), cells were washed
81 once in the assay medium containing 10 mM MOPS buffer, 0.1 mM NH₄Cl, 1.3 mM KCl, 1 mM
82 Na-β-glycerophosphate, 0.12 mM MgSO₄, 1 mM sodium acetate, and 1 µg/mL resazurin at pH
83 6.8. Sodium fumarate was added to the assay medium after autoclaving to a final concentration of
84 1 mM from a filter-sterilized stock solution.

85 ***Cell surface thiol quantification.*** The thiol concentration at the cell surface of exponentially
86 grown *G. sulfurreducens* was quantified after reaction with (qBBr) by fluorescence spectroscopy
87 on a Photon Technology International (PTI) Quantamaster fluorometer as described in Joe-Wong
88 et al.³⁴ Cells that were washed with the assay medium were diluted to an OD₆₀₀ of 0.015 – 0.04 in
89 the assay medium, and 7 – 8 mL of cell suspension were distributed among 15 mL N₂-flushed,
90 acid-washed serum vials. Microliter volumes of a qBBr stock solution that was prepared in anoxic
91 Milli-Q were added to cell suspensions (8 mL final volume) under N₂ atmosphere and crimp sealed
92 with butyl rubber septa. Cell suspensions were mixed with qBBr for 2 hours and those that did not

93 remain anoxic throughout the experiment (shown by the resazurin indicator) were not analyzed. A
94 2 mL aliquot was extracted with a syringe and quickly dispensed into a polystyrene fluorometer
95 cuvette (Fisher Scientific). A fluorescence spectrum was immediately measured from 400 to 500
96 nm (380 nm excitation), and the fluorescence at 470 nm was selected for analysis. While only 1
97 scan is necessary per sample, the fluorescence measurement is stable in air up to 4 scans of ~1.5
98 min duration.

99 ***Hg(II) exposure assays.*** For Hg(II) sorption/methylation experiments, 7.2 mL of cell suspension
100 in assay medium were transferred to N₂-flushed, acid-washed 15 mL borosilicate glass serum vials
101 under a stream of N₂ gas in the headspace. To achieve final Hg(II) concentrations of 0 – 200 nM,
102 0.8 mL of 10 times concentrated Hg(II) stock solution prepared in anoxic Milli-Q water was added
103 to the cell suspension so that the final volume was 8 mL. After Hg(II) addition, vials were crimp
104 sealed with rubber septa. A 10 mM Hg(NO₃)₂ stock solution in 1% HNO₃ (trace metal grade) was
105 used for all exposure assays and stored at 4 °C. For HR-XANES samples, the above procedure was
106 replicated, but the final volume of cell suspension with Hg(II) addition was 50 mL in 100 mL acid-
107 washed serum bottles. All assays involving Hg(II) were mixed for 2 hours at 150 rpm in the dark
108 at room temperature. Vials that did not remain anoxic during the exposure assays (as determined
109 by the resazurin indicator) were not analyzed. When the effect of qBBr was tested (i.e., blocking
110 cell surface thiols), a microliter volume of qBBr stock solution prepared in anoxic Milli-Q was
111 added to the cell suspension and allowed to mix for 2 hours prior to Hg addition. When the effect
112 of Cys was tested, a microliter volume of Cys stock prepared directly before use was pre-
113 equilibrated with Hg(II) in anoxic Milli-Q for 1 hour at 10 times the final desired concentration.
114 The pre-equilibrated Hg(II)-Cys solution was then diluted by a factor of 10 upon addition to cell
115 suspensions.

116 **Total and methyl-Hg measurements.** Aliquots (700 μ L) for total and dissolved Hg(II) and MeHg
117 were collected by syringe after the 2 hour mixing period with Hg (\pm qBBr/Cys), preserved in
118 \sim 0.5% HCl in amber borosilicate glass vials and placed in the freezer until analysis. At least 3
119 replicates from independent experiments were measured for each sample. Total Hg measurements
120 were made on a Lumex RA-915M Mercury Analyzer with Pyrolyzer PYRO-915+ (Solon, OH).³⁵
121 Between 50 to 200 μ L of liquid sample was pipetted onto \sim 100 mg of activated carbon in the
122 quartz sample boat, which was placed into the thermal decomposition chamber reaching a
123 temperature of \sim 800 $^{\circ}$ C. The Hg in the sample was atomized and brought to the analysis cell by a
124 steady air flow. The total Hg concentration was obtained by atomic absorption spectroscopy at 254
125 nm with Zeeman correction for background absorption. The recovery was within $100 \pm 5\%$ for a
126 50 nM control solution made in the assay medium. For MeHg analysis, samples were distilled by
127 a Tekran 2750 gas manifold and heating system and analyzed by cold vapor atomic fluorescence
128 spectroscopy (CVAFS) with a Tekran 2700 Methylmercury Analysis System as described in US
129 EPA Method 1630. All MeHg controls and references for calibration were prepared from a Brooks
130 Rand 1 ppm MeHg stock solution. Blanks in the assay medium (\pm 50 nM Hg), MeHg spiked
131 samples, and MeHg references were run every 10 – 15 samples. In addition, controls were made
132 in the assay medium to test recovery after distillation and derivatization. The recovery was within
133 $100 \pm 10\%$.

134 **HR-XANES sample collection and measurements.** The bacterial density and the initial and total
135 recovered Hg concentration for each sample measured by HR-XANES is provided in Table S2.
136 After mixing with Hg(II) for 2 hours (\pm Cys/qBBr), the cell suspension was washed twice with
137 anoxic 0.1 M NaClO₄. After the final wash, the cells were resuspended in \sim 200 μ L anoxic 0.1 M
138 NaClO₄ and pipetted into a 1.5 mL microfuge tube that was fitted with an EMD Millipore

139 centrifugal filter unit (Mfr # UFC510024). We switched out the filter that was provided in the unit
140 with a 0.2 μm cellulose acetate filter (Whatman) that we cut with a ~ 7 mm diameter hole punch.
141 The cell suspension was centrifuged at 10,000 g for 5 minutes, collecting the cell pellet on the
142 filter and allowing excess moisture to pass through the filter. The filter with cell pellet was
143 sandwiched between pieces of Kapton tape, quickly plunged into LN_2 , and remained frozen until
144 analysis with HR-XANES.

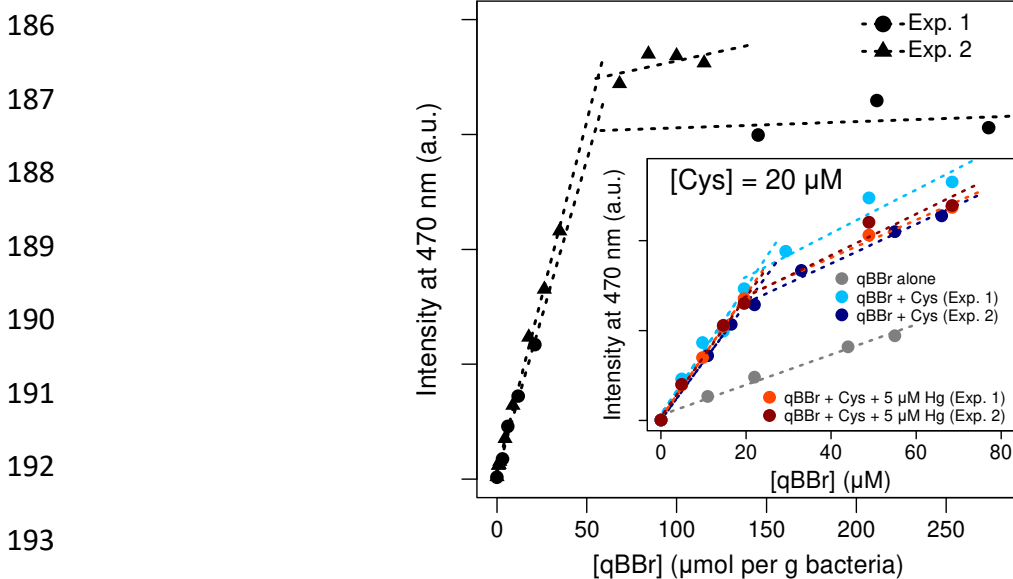
145 The HR-XANES data were collected at the European Synchrotron Radiation Facility
146 (ESRF) at beamline BM16 FAME-UHD. All measurements were performed in high energy
147 resolution fluorescence detection (HERFD) mode with 5 spherically bent Si(111) crystal analyzers
148 (bending radius = 1 m, crystal diameter = 0.1 m). The Hg $L\alpha_1$ fluorescence line was measured
149 with a silicon drift detector (SDD, Vortex EX-90). The beam size was $100 \mu\text{m} \times 200 \mu\text{m}$. The
150 monochromator was calibrated with a Se reference foil by assigning the zero value of the first
151 derivative to the Se K-edge energy (12,658 eV), and a HgCl_2 powder was scanned at the start of
152 each experiment to maintain relative energy calibration. The powder standards were finely ground,
153 diluted to ~ 0.5 wt% with boron nitride, pressed into ~ 5 mm diameter pellets, and loaded onto a
154 copper sample holder. The liquid reference standards were pipetted into a copper sample holder
155 sealed on two ends with Kapton tape that was quickly plunged into LN_2 to minimize contact of the
156 liquid with the copper as well as prevent the formation of ice. The bacterial samples were shipped
157 to the ESRF on dry ice (< 48 hours in transit) and kept frozen during analysis. The frozen bacterial
158 samples were quickly fixed onto copper sample holders with grease and plunged into liquid
159 nitrogen to prevent thawing. All references and bacterial samples were measured at 10 – 15 K with
160 some references also being measured at room temperature for comparison. The beam position on
161 the sample was moved after every scan (duration ~ 35 minutes); however, no beam damage was

162 observed on repeat scanning locations. The data normalization was executed in Athena³⁶ while
163 peak fitting was performed in Larch.³⁷ Details on the preparation of Hg reference standards for
164 HR-XANES is provided in a previous publication.¹⁶

165 **Results and Discussion**

166 ***Quantification of cell surface thiols.*** The fluorophore monobromo(trimethylammonio)bimane
167 (qBBr) binds strongly and irreversibly to thiols via nucleophilic substitution (S_N2) and has been
168 used to estimate thiol concentration in LMW ligands and macromolecular dissolved natural
169 organic matter.³⁴ qBBr is a relatively large and positively charged molecule and thus does not
170 penetrate cell membranes (outer and cytoplasmic). It can therefore be used to quantify thiols at
171 cell surfaces, which include thiols that are associated with the outer membrane or extracellular
172 polymeric substance (EPS).^{34, 38-41} Furthermore, a qBBr titration accurately estimates the
173 concentrations of thiols, such as Cys and glutathione (GSH), in the assay medium from this study
174 (Figure S1). Aliquots of *G. sulfurreducens* suspensions that were harvested in exponential growth
175 phase were titrated with increasing concentrations of qBBr and mixed anaerobically for 2 hours,
176 after which the fluorescence intensity at 470 nm was measured and plotted against the qBBr
177 concentration (Figure 1). The intersection of the two best-fit lines (i.e., saturation of all accessible
178 thiols from reactions with qBBr) from independent experiments revealed a consistent average thiol
179 concentration at the cell surface of $55.5 \pm 1.3 \mu\text{mol/g}$ bacteria (wet weight) or $\sim 2 \times 10^8$ thiols/cell.
180 The measurement of cell surface thiol concentration is steady up to 4 hours of mixing, and our
181 measured value agrees well with a recent study that determined the surface thiol concentration of
182 *G. sulfurreducens* by potentiometric titration.²² In addition, cell suspensions titrated with qBBr
183 remain anoxic (as determined by the resazurin indicator) for up to 4 hours, which implies that cells

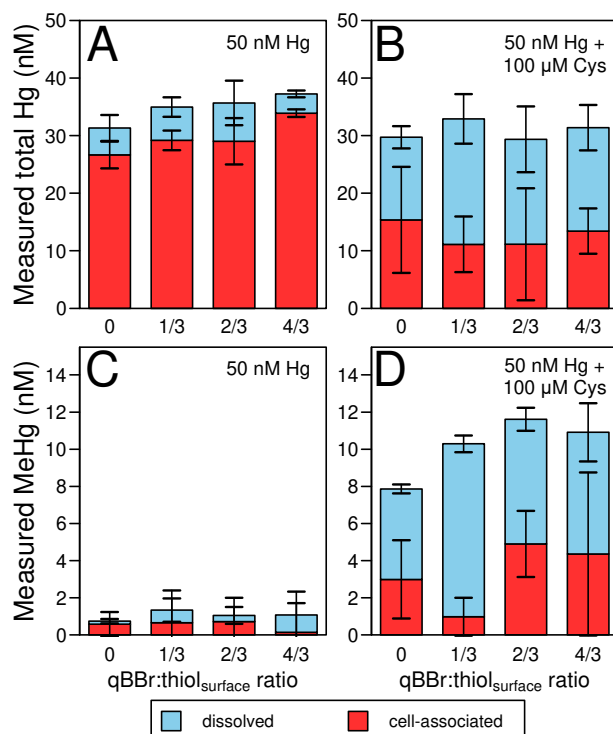
184 retain an active metabolism to reduce the assay medium even after the blocking of surface thiols
185 by qBBr.



194 **Figure 1.** The fluorescence intensity of *G. sulfurreducens* cell suspension measured at 470 nm
195 (excitation: 380 nm) as a function of the added qBBr concentration after a 2-hour exposure to
196 estimate surface thiol density. The qBBr concentration is normalized to the cell density (g/L) for
197 each experiment. The intersection of the two best-fit lines within each experiment indicates a cell
198 surface thiol concentration of 56.4 and 54.6 μmol thiol per g bacteria (wet weight), respectively.
199 Inset: qBBr titrations in the absence of bacteria of the assay medium alone (gray), with 20 μM Cys
200 (light/dark blue), and with 20 μM Cys and then mixing with 5 μM Hg for one additional hour
201 (light/dark red). The intersection of the two best-fit lines within each experiment estimates a Cys
202 concentration of 20.0 ± 0.3 μM and 21.4 ± 1.6 μM with and without the addition of Hg,
203 respectively. Thus, Hg addition does not break the qBBr-thiol bond. Thermodynamic calculations
204 predict ~11 μM free Cys in the presence of 5 μM Hg (the remainder forming Hg(Cys)₂ and HgCys)
205 in the absence of qBBr.¹⁶

206
207 **Hg(II) binding to cell surface thiols and their impact on MeHg production.** Once the thiol reacts
208 with qBBr, the qBBr-thiol bond cannot be broken by Hg(II) addition (Figure 1 inset). Thus, qBBr
209 can be used to selectively block cell surface thiols in Hg uptake and methylation assays. We tested
210 how the blocking of surface thiols by qBBr as well as Cys addition affected cellular Hg(II) sorption
211 and MeHg production after exposing cells to Hg(II) with and without Cys for 2 hours (Figure 2).
212 The total concentration of cell surface thiols (~56 μmol per L) is approximately 1000 times greater

213 than the total added Hg(II) concentration for these experiments (50 nmol per L). The addition of
 214 qBBr at 1/3, 2/3 and 4/3 the concentration of the total cell surface thiols to block 1/3, 2/3 and all
 215 accessible cell surface thiols, respectively, had no effect on the sorption or methylation of 50 nM
 216 total Hg (Figure 2A,C). Regardless of the qBBr concentration added, the sorbed Hg(II) was ~90%
 217 of the total recoverable Hg(II) (Figure 2A). In addition, cells exposed to 50 nM Hg(II) only
 218 produced 1 – 2 nM total MeHg after 2 hours regardless of qBBr addition (Figure 2C). We note
 219 that the total recovered Hg (dissolved + cell-associated) does not add up to the initial added Hg
 220 after mixing both in the presence and absence of added cysteine (Figures 2A and 2B). The lower
 221 Hg recovery is likely due to Hg(II) reduction by the cytochromes of *G. sulfurreducens* and the loss
 222 of volatile Hg(0) into the headspace of the serum vial, which is known to occur under the Hg to
 223 cell ratios of this study.⁴²

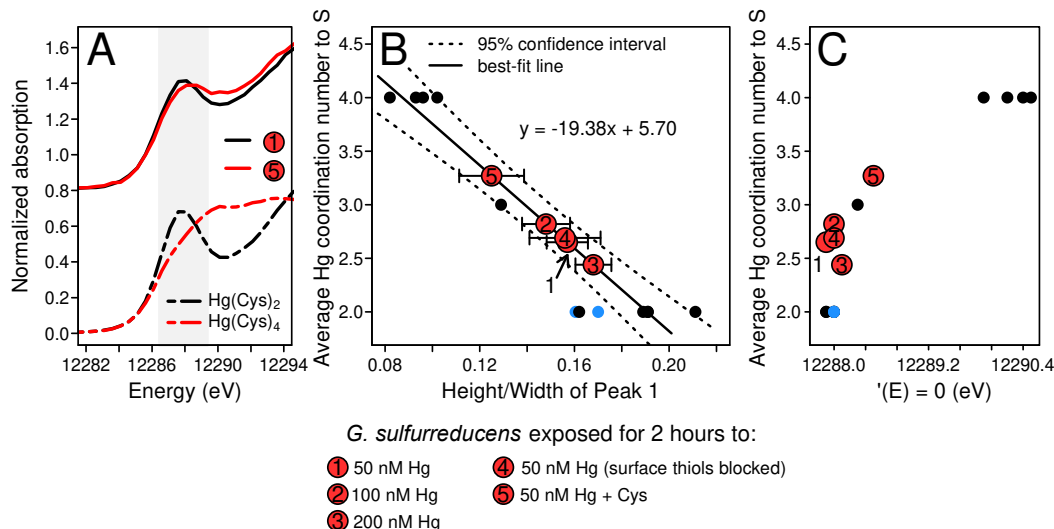


234 **Figure 2.** The dissolved and cell-associated (A,B) total Hg as well as (C,D) MeHg measured as a
 235 function of added qBBr to cell surface thiol ratio after exposure of *G. sulfurreducens* to (A,C) 50
 236 nM Hg and (B,D) 50 nM Hg + 100 μM Cys for 2 hours. The cells were incubated with the specified
 237 qBBr concentration for 2 hours prior to Hg/Cys addition.

238 As expected, the addition of 100 μM Cys and 50 nM total Hg(II) to *G. sulfurreducens*
239 drastically enhanced the total MeHg production (Figure 2D). In addition, the blocking of cell
240 surface thiols with qBBr did not significantly affect Hg(II) sorption or methylation in the presence
241 of added Cys (Figure 2B,D). However, the presence of Cys enhanced the fraction of dissolved Hg
242 in the exposure medium, regardless of the fraction of surface thiols blocked by qBBr, which is
243 likely due to a combination of efficient MeHg export from the cell^{13, 14} as well as increased Hg(II)
244 solubility (i.e., not cell-associated) due to its complexation with Cys in the exposure medium. Our
245 findings suggest that the majority of cell surface thiols do not influence Hg(II) uptake and
246 methylation, both in the presence and absence of added Cys. In addition, due to consistent MeHg
247 production in the presence and absence of qBBr, these results confirm that cell physiology was
248 minimally influenced by the inhibition of cell surface thiols. It is possible that a small fraction of
249 surface thiols that are embedded deeper within the outer membrane (e.g. some cysteine residues
250 of outer membrane proteins) could react with Hg but not with qBBr molecules due to size and/or
251 steric hindrance. Therefore, the involvement of cell surface thiols in Hg methylation cannot be
252 ruled out completely. However, blocking the majority of surface thiols from binding Hg appears
253 to have no effect on Hg methylation. Due to the abundance of qBBr-blocked surface thiols (~ 56
254 $\mu\text{mol per L}$) in comparison to the total Hg concentration (50 nmol per L) in this study, bacterial
255 surface thiols may be a large sink for Hg(II) in natural environments.

256 ***Hg(II) coordination environment in Hg-methylating bacterium.*** To identify the cell-associated
257 Hg(II) species in actively Hg-methylating bacteria, we probed samples of *G. sulfurreducens* that
258 were exposed for 2 hours to a range of Hg concentrations (50 – 200 nM) with and without cell
259 surface thiol blocking and Cys addition using Hg L₃-edge HR-XANES spectroscopy (Figure S2).
260 The results show that all detectable Hg(II) associated with the bacteria herein is bound to S with

261 the possibility of mixed Hg bonding to S and N/O in some samples (described later). The greatest
 262 variation in the cellular Hg coordination environment was found in cells exposed to Cys (Figure
 263 S2C).



271 **Figure 3.** (A) Normalized Hg L₃-edge HR-XANES of aqueous standards of Hg(Cys)₂ (pH = 3)
 272 and Hg(Cys)₄ (pH = 11) as well as cell pellets of *G. sulfurreducens* exposed to 50 nM Hg (1) and
 273 50 nM Hg with 100 μM Cys (5) for 2 hours. (B) The ratio of the height to the width of the
 274 deconvoluted near-edge HR-XANES Gaussian peak (Peak 1) plotted against the known average
 275 Hg coordination number to S for Hg standards from this study and from Manceau et al.^{26,44} (black
 276 dots). A description of the spectral deconvolution method is provided in the SI (Part S1). A best-
 277 fit line with 95% confidence interval was calculated from the black dots only. The blue dots
 278 represent Hg(Cys)₂ and Hg(GSH)₂ made at pH 7.5 from Bourdineaud et al., where an
 279 amine/carboxyl group is also included in the coordination sphere (i.e., Hg[(SR)₂ + (N/O)₁₋₂]).²⁷
 280 The red circles represent sample spectra of *G. sulfurreducens* exposed to 50 nM Hg, 100 nM Hg,
 281 200 nM Hg, 50 nM Hg with surface thiols quantitatively blocked by qBBr, and 50 nM Hg with
 282 100 μM Cys for 2 hours. The error bars depict the calculated uncertainty of the height/width
 283 parameter from the fit model. (C) The average Hg coordination number to S of Hg standards and
 284 samples from subplot B plotted against the energy in the edge region at which the first derivative
 285 of the HR-XANES is equal to zero ($\mu'(E) = 0$).

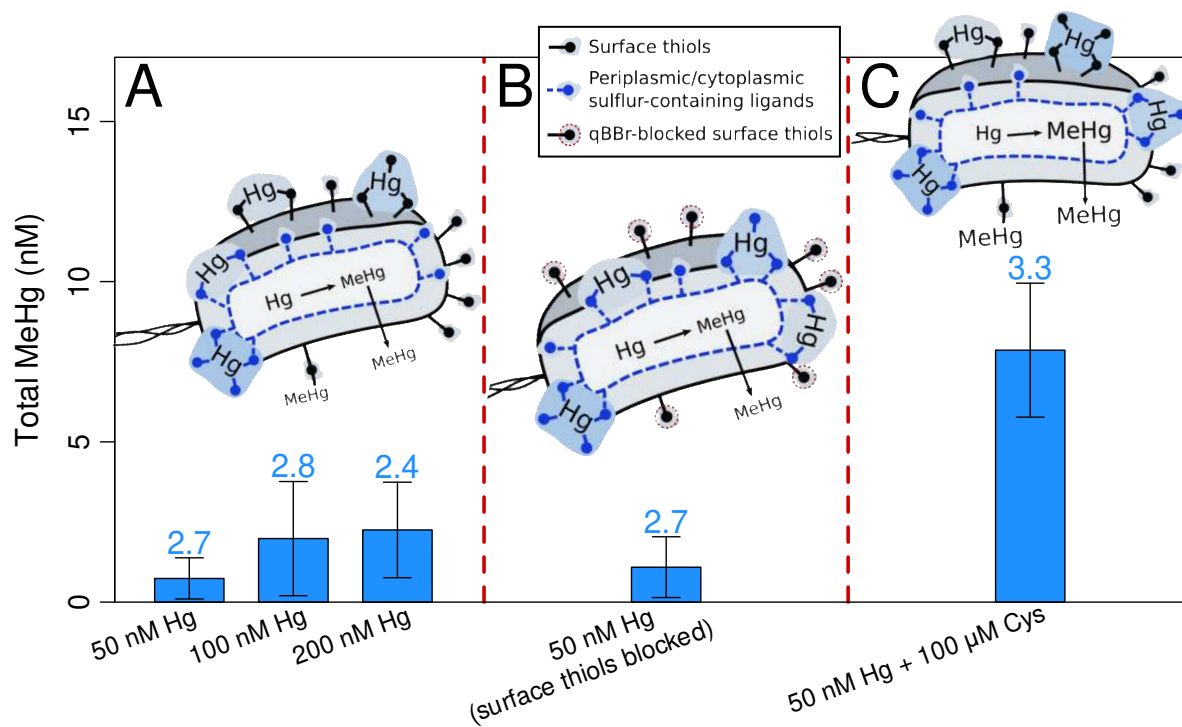
286
 287 Detailed metal coordination environments in unknown samples are typically obtained by
 288 comparing their XANES spectra with those of structurally well-characterized models. A similar
 289 attempt to identify the Hg coordination environments in this study by linear combination fit is not
 290 appropriate because our library of standards does not entirely match the experimental spectra. HR-

291 XANES is highly sensitive to structural distortions and higher coordination shells,⁴³ which likely
292 explains the dissimilarities between the spectra of dilute Hg(II) species that form in the bacteria
293 from this study and the pure aqueous and crystalline Hg(II) standards of our library. However, the
294 average Hg(II)-S coordination number can be estimated by examining the peak intensity and width
295 of the lowest energy transition in Hg L₃-edge HR-XANES spectra, which corresponds to the Hg
296 2p_{3/2} to hybridized Hg 6s5d transition.⁴⁴ A sharp and intense near-edge peak is indicative of linear
297 2-coordinate Hg-S bonds (see Hg(Cys)₂ of Figure 3A).³⁰ Deviations from linearity caused by
298 distortion or an additional atom in the coordination sphere (e.g., N, O, or S) produce a smaller peak
299 amplitude.²⁹ Manceau et al. obtained a Hg L₃-edge HR-XANES spectrum of a trigonal Hg(SR)₃
300 complex, which has a very small near-edge peak,⁴⁴ while spectra of Hg bound to 4 S atoms in
301 tetrahedral geometry (i.e., Hg(SR)₄ and β-HgS) lack a visible near-edge peak (see Hg(Cys)₄ of
302 Figure 3A).^{16, 28, 30, 44}

303 We have developed a method that involves spectral deconvolutions of Hg L₃-edge HR-
304 XANES spectra of many compounds with Hg-S coordination to extract Hg coordination
305 information. Specifically, we deconvoluted the spectra into 4 Gaussian peaks and an error function
306 and further analyzed the Gaussian peak in the near-edge, hereafter referred to as Peak 1 (SI Part
307 S1). A standard curve was created by plotting the ratio of the height to the width (2σ) of Peak 1
308 against the known average Hg-S coordination number using spectra from this study, Manceau et
309 al.,^{26, 44} and Boudineaud et al.²⁷ (Figure 3B). Because the Hg-S₂, Hg-S₃, and Hg-S₄ species lie in
310 distinct regions of the standard curve in Figure 3B, this curve can estimate the average Hg(II)
311 coordination number to S in samples that contain Hg predominantly bound to S. However, the
312 curve is not very sensitive to mixed coordination environments of S and N/O. This is shown by
313 comparing the height to width ratio of Peak 1 for the Hg-S₂ species and the two Hg[(SR)₂ + NH₂]

314 species (blue dots; Figure 3B), which lie in the same range. However, it is possible to differentiate
315 Hg[(SR)₂ + (N/O)₁₋₂] binding from mixed Hg-S₂ and Hg-S₃/S₄ binding using the energy of Peak 1
316 (defined as the energy in the edge region at which the HR-XANES derivative equals zero), which
317 is similar for Hg-S₂ and Hg[(SR)₂ + (N/O)₁₋₂] species but differs between Hg-S₂ and Hg-S₃/S₄
318 species (Figure 3C). We note that Hg-C bonding due to MeHg formation does not impact the
319 interpretation of the results in this study because our MeHg analysis shows that cell-associated
320 MeHg (likely as MeHg-Cys²⁹) is < 20% of the total cell-associated Hg for the sample involving
321 Cys and negligible (< 2%) for the other 4 samples.

322 Our analysis of the samples of *G. sulfurreducens* that were exposed to 50 – 200 nM total
323 Hg indicates that the cell-associated Hg is bound to S with an average coordination number of 2 –
324 3 (range includes 95% confidence interval and consideration of Hg[(SR)₂ + (N/O)₁₋₂] binding;
325 Figure 3B). This average Hg coordination number does not change when the surface thiols are
326 quantitatively blocked by qBBr (Figure 3B). In contrast, the sample with Cys addition has a
327 significantly larger Hg coordination number to S of 3.3 ± 0.2 (Figure 3B). This sample also has a
328 near-edge HR-XANES peak energy that is 0.5 eV greater than the other samples (Figure 3C). This
329 shift in energy confirms independently a larger Hg coordination number to S and provides further
330 evidence that the sample with Cys addition is significantly different than the others. Finally, there
331 is additional evidence for mixed Hg[(SR)₂ + (N/O)₁₋₂] coordination in the samples of *G.*
332 *sulfurreducens* exposed to 100 nM Hg as well as 50 nM Hg with the surface thiols blocked due to
333 a left-shifted edge energy above the near-edge peak (Figure S2A and S2B).²⁹ Mixed Hg[(SR)₂ +
334 (N/O)₁₋₂] binding environments occur when Hg binds to LMW thiols of biological origin at neutral
335 pH (i.e., GSH).²⁷ Due to the abundance of LMW thiols like GSH in bacteria,⁴⁵ Hg[(SR)₂ + (N/O)₁₋₂]
336] binding could be a result of increased Hg binding to LMW thiols.



337 **Figure 4.** The total MeHg concentration (nM) produced by *G. sulfurreducens* after exposure to 50
 338 – 200 nM total Hg for 2 hours is plotted with the average Hg coordination number to S in the cell
 339 pellet for each sample (blue numbers above bars; determined from Figure 3) to understand the
 340 relationship between cellular Hg coordination and MeHg production. We did not determine the
 341 localization of cell-associated Hg in this study; thus, the illustration merely proposes the Hg
 342 distribution among surface thiols and periplasmic/cytoplasmic S-containing ligands while
 343 satisfying the measured average cell-associated Hg coordination number to S. (A) The cell-
 344 associated Hg is coordinated on average to between 2 and 3 S atoms considering the 95%
 345 confidence interval and the possibility of mixed Hg[(SR)₂ + (N/O)₁₋₂] binding causing a slight
 346 overestimation of the Hg-S coordination number. These conditions are linked to relatively low
 347 MeHg production. (B) When surface thiols are completely blocked by qBBR, the average Hg
 348 coordination number to S is also 2 – 3 and MeHg production is unchanged. Because the surface
 349 thiols are fully blocked, Hg is likely distributed among periplasmic/cytoplasmic S-containing
 350 ligands. (C) When 50 nM Hg is added with 100 μM Cys, the cell-associated Hg is coordinated on
 351 average to 3.3 S atoms, and MeHg production is relatively high. Due to the high MeHg
 352 concentration and requirement that Hg be in the cytosol for MeHg production, Hg must be
 353 coordinated to some intracellular (periplasmic/cytoplasmic) ligands.

354
 355 **Implications for Hg biouptake and methylation.** Our results indicate that a vast majority of cell
 356 surface thiols on a Hg-methylating organism are not involved in Hg(II) biouptake and methylation.
 357 In addition, we show that the cell-associated Hg(II)-S coordination number is positively correlated
 358 with MeHg production, as opposed to the ability of cell surface thiols to bind and retain Hg (Figure
 359 4). When the average Hg(II) coordination number to S is low (< 3), MeHg production is also low

360 (Figure 4A), regardless of whether the cell surface thiols are blocked by qBBr (Figure 4B).
361 Likewise, the addition of Hg that was pre-equilibrated with Cys led to the highest cell-associated
362 Hg coordination number to S (3.3) and the highest MeHg production by *G. sulfurreducens* (Figure
363 4C). In order to satisfy an average coordination number to S of 3.3, Hg can exist either as
364 predominantly Hg-S₃ or a mixture of Hg-S₂, Hg-S₃, and Hg-S₄ with the likely presence of Hg-S₄
365 in both cases to push the coordination number above 3. The correlation between Hg-S₃/S₄ species
366 and MeHg production could be due to the species' enhanced bioavailability or connection to the
367 form of Hg that is methylated. An indirect reason could also lead to enhanced Hg methylation,
368 such as the formation of an intermediate complex, which is manifested by increased Hg-S
369 coordination number. Regardless of the exact mechanism, the formation of Hg species with
370 coordination numbers to S at or above 3 must either induce or be byproducts of the conditions
371 favorable for MeHg production.

372 Cell-associated Hg-S₄ species would likely be comprised of Hg binding to inorganic sulfur
373 (i.e., β -HgS), as opposed to organic sulfur (i.e., Hg(SR)₄). Inorganic Hg(II)-sulfides form readily
374 with sulfide ions,^{46, 47} can precipitate extracellularly (and potentially intracellularly) in non-
375 dissimilatory sulfate reducing bacterial suspensions without sulfide additions,¹⁶⁻¹⁸ and can even
376 form directly from Hg(II)-thiol complexes.^{30, 48} In contrast, the formation of Hg(SR)₄ at neutral
377 pH is highly unfavorable.⁴⁹ It is notable that the HR-XANES do not indicate cell-associated bulk
378 β -HgS or Hg(SR)₄ for any bacteria sample. However, small cell-associated Hg-S clusters with β -
379 HgS-like local Hg coordination (i.e., analogous to Fe-S clusters), as described by Manceau et al.,^{27,}
380 ⁵⁰ are possible, especially due to the low Hg concentrations associated with the bacteria samples.
381 Because Hg-S₄ is most likely present in the sample with Cys addition and *G. sulfurreducens* is
382 known to degrade exogenous Cys into sulfide under identical exposure conditions as this study,¹⁷

383 the nucleation of Hg-S nanoclusters with β -HgS-like local coordination is possible, as suggested
384 previously.^{16, 17} If cell-associated Hg is present as Hg-S₃, we predict the trigonal coordination of
385 Hg with 3 structurally connected thiols, which is the most stable Hg-S₃ species at physiological
386 pH⁴⁹ and has been observed in proteins (e.g., Hg-MerR in organisms with the mer operon).⁵¹ The
387 most stable and common Hg(II)-thiol complexes in biological samples are linear, 2-coordinate.⁵²
388 Therefore, the cell-associated Hg-S₂ species that we observe are likely Hg(SR)₂, with the
389 possibility of mixed Hg[(SR)₂ + (N/O)₁₋₂] coordination.

390 Curiously, if the Hg-S₄ species is directly related to Hg methylation, it is highly unlikely
391 that this is the species that accepts a methyl group to become MeHg because the Hg coordination
392 sphere is already fully occupied with 4 S atoms. Hg methylation by HgcAB is depicted in the
393 literature as the donation of a methyl carbanion (CH₃⁻) from HgcA to a Hg(SR)₂ complex, using
394 HgcB as an electron donor to reduce the corrinoid cofactor of HgcA.^{52, 53} However, the assumption
395 that Hg(SR)₂ accepts a CH₃⁻ group is solely due to the previous understanding that Hg(SR)₂ is the
396 predominant form of Hg in cells.^{52, 54} An interesting study would explore the possibility of the
397 methylation of Hg-S₃ or Hg-S₄ species, for example, considering a change in Hg coordination by
398 ligand exchange reactions so that the Hg coordination sphere could accept a methyl group. Site-
399 directed mutagenesis of 3 conserved Cys residues in *hgcB* revealed that at least two (i.e., Cys73
400 and Cys94 or Cys95) are required for Hg methylation,⁵³ and it is possible that 2 or 3 of these Cys
401 residues bind Hg while a methyl group is transferred from HgcA. A Hg(SR)₃ binding structure,
402 analogous to Hg-MerR, would be highly stable⁵¹ and should outcompete Hg-S₂ species and
403 possibly even inorganic Hg-S₄ species. The coordination of Hg to 3 Cys residues of HgcB could
404 itself contribute to our observation of a possible Hg-S₃ species, although the reported abundance
405 of HgcAB in cells is very low.^{55, 56}

406 The *hgcAB* gene cluster responsible for MeHg production is expressed constitutively and
407 is not responsive to Hg.⁵⁷ Therefore, Hg biouptake to the cytosol so that Hg reaches the HgcAB
408 active sites is likely the foremost cause for Hg-methylation. In light of the previous evidence
409 attributing MeHg production to the passive diffusion of neutral Hg(II)-sulfide species,⁸⁻¹¹ it is
410 possible that Cys leads to enhanced MeHg production due to the formation of cell-associated
411 Hg(II)-sulfide species (i.e., Hg-S₄) that can passively diffuse through the cell membrane layers.
412 The adsorption of Hg(II) to cell surface thiols has been proposed to immobilize Hg(II) against
413 biouptake.⁵⁸⁻⁶⁰ Thus, the formation of highly stable Hg-S₄ species may enable Hg(II) to bypass
414 binding to cell surface thiols, promoting Hg(II) biouptake into the cytosol. This hypothesis
415 supports our finding that blocking cell surface thiols had no effect on Hg(II) methylation in the
416 presence of added Cys. In addition, recent evidence suggests that the biodegradation of Cys to
417 sulfide and the coexistence of these reduced sulfur species is necessary for Hg(II) uptake by
418 *Escherichia coli* exposed to excess Cys.¹⁶ The necessity of Hg(II)-sulfide species formation for
419 biouptake in the presence of excess Cys can explain the observation that Hg(II) biouptake by *G.*
420 *sulfurreducens* is enhanced by Cys but inhibited by similar thiols that are not readily degradable
421 to sulfide (e.g., GSH and penicillamine) under otherwise identical conditions.¹³ Lastly, at high Cys
422 concentrations¹⁴ or in a mutant *G. sulfurreducens* strain that lacks outer membrane proteins
423 ($\Delta omcBESTZ$),¹⁵ Hg(II) uptake and methylation in the presence of Cys is inhibited, which could
424 be related to the inability to degrade enough Cys to enable Hg(II)-sulfide species (i.e., Hg-S₄)
425 formation.

426 This study indicates that the average cell-associated Hg coordination number to S is
427 influential to MeHg production by a model Hg-methylating bacterium while the abundance of cell
428 surface thiols capable of binding Hg(II) is not. We propose that the Hg-S₃/Hg-S₄ species, whose

429 formation correlates with MeHg production, are highly stable and sufficiently small Hg(II)-sulfide
430 clusters with enhanced biouptake potential (possibly by passive diffusion). In the cytosol, the Hg-
431 S₃/Hg-S₄ species may undergo a ligand exchange reaction, potentially with the 3 Cys residues of
432 HgcB, prior to the addition of a methyl group to the coordination sphere to form MeHg. The link
433 between Hg-S₃/Hg-S₄ species formation and Hg(II) biouptake as well as the methylation of highly
434 stable Hg(II) species should be explored further. In addition, by identifying unexpected cell-
435 associated Hg-S₃/Hg-S₄ species, we demonstrate the importance of characterizing cell-associated
436 Hg coordination chemistry during Hg biouptake and methylation assays. Experimental approaches
437 to directly obtain coordination information, such as HR-XANES spectroscopy, have the potential
438 to shed light on the bioavailability of other metal species as well.

439

440 **Acknowledgements**

441 This work is supported by the National Science Foundation under grant EAR-1424899 and the
442 Scott Vertebrate Fund of the Department of Geosciences, Princeton University. The experiments
443 were performed on beamline BM16 – UHD-FAME – at the European Synchrotron Radiation
444 Facility (ESRF), Grenoble, France. The FAME-UHD project is financially supported by the
445 French “grand emprunt” EquipEx (EcoX, ANR-10-EQPX-27-01), the CEA-CNRS CRG
446 consortium, and the INSU CNRS institute. We are grateful for the beamline assistance of Dr.
447 Mauro Rovezzi at BM16. We also thank Dr. Jeffra Schaefer for supplying the *G. sulfurreducens*
448 strain as well as providing helpful information on the anaerobe culture and Hg methylation assays.
449 We appreciate the assistance of Xiaoshuai He during MeHg analysis. Finally, we thank Dr. Alain
450 Manceau for helpful comments in reviewing this manuscript.

451

452 **Supporting Information**

453 Thiol quantification control experiments, HR-XANES spectra of bacterial samples, protocol for
454 spectral deconvolution of HR-XANES, deconvoluted HR-XANES spectra, parameters of
455 deconvoluted HR-XANES spectra.

456

457 **References**

- 458 1. Gilmour, C. C.; Bullock, A. L.; McBurney, A.; Podar, M.; Elias, D. A., Robust mercury
459 methylation across diverse methanogenic archaea. *Mbio* **2018**, *9*, (2).
460
- 461 2. Podar, M.; Gilmour, C. C.; Brandt, C. C.; Soren, A.; Brown, S. D.; Crable, B. R.;
462 Palumbo, A. V.; Somenahally, A. C.; Elias, D. A., Global prevalence and distribution of genes
463 and microorganisms involved in mercury methylation. *Science Advances* **2015**, *1*, (9).
464
- 465 3. Gilmour, C. C.; Podar, M.; Bullock, A. L.; Graham, A. M.; Brown, S. D.; Somenahally,
466 A. C.; Johs, A.; Hurt, R. A.; Bailey, K. L.; Elias, D. A., Mercury methylation by novel
467 microorganisms from new environments. *Environmental Science & Technology* **2013**, *47*, (20),
468 11810-11820.
469
- 470 4. Parks, J. M.; Johs, A.; Podar, M.; Bridou, R.; Hurt, R. A.; Smith, S. D.; Tomanicek, S. J.;
471 Qian, Y.; Brown, S. D.; Brandt, C. C.; Palumbo, A. V.; Smith, J. C.; Wall, J. D.; Elias, D. A.;
472 Liang, L. Y., The genetic basis for bacterial mercury methylation. *Science* **2013**, *339*, (6125),
473 1332-1335.
474
- 475 5. Liem-Nguyen, V.; Skyllberg, U.; Björn, E., Thermodynamic modeling of the solubility
476 and chemical speciation of mercury and methylmercury driven by organic thiols and micromolar
477 sulfide concentrations in boreal wetland soils. *Environmental Science & Technology* **2017**, *51*,
478 (7), 3678-3686.
479
- 480 6. Morel, F. M. M.; Kraepiel, A. M. L.; Amyot, M., The chemical cycle and
481 bioaccumulation of mercury. *Annu Rev Ecol Syst* **1998**, *29*, 543-566.
482
- 483 7. Skyllberg, U., Competition among thiols and inorganic sulfides and polysulfides for hg
484 and meh_g in wetland soils and sediments under suboxic conditions: Illumination of controversies
485 and implications for meh_g net production. *J Geophys Res-Bioge* **2008**, *113*.
486
- 487 8. Benoit, J. M.; Gilmour, C. C.; Mason, R. P., Aspects of bioavailability of mercury for
488 methylation in pure cultures of *desulfobulbus propionicus* (1pr3). *Applied and Environmental*
489 *Microbiology* **2001**, *67*, (1), 51-58.
490

- 491 9. Benoit, J. M.; Gilmour, C. C.; Mason, R. P., The influence of sulfide on solid phase
492 mercury bioavailability for methylation by pure cultures of *Desulfobulbus propionicus* (1pr3).
493 *Environmental Science & Technology* **2001**, *35*, (1), 127-132.
494
- 495 10. Benoit, J. M.; Gilmour, C. C.; Mason, R. P.; Heyes, A., Sulfide controls on mercury
496 speciation and bioavailability to methylating bacteria in sediment pore waters. *Environmental*
497 *Science & Technology* **1999**, *33*, (6), 951-957.
498
- 499 11. Drott, A.; Lambertsson, L.; Björn, E.; Skyllberg, U., Importance of dissolved neutral
500 mercury sulfides for methyl mercury production in contaminated sediments. *Environmental*
501 *Science & Technology* **2007**, *41*, (7), 2270-2276.
502
- 503 12. Schaefer, J. K.; Szczuka, A.; Morel, F. M. M., Effect of divalent metals on hg(ii) uptake
504 and methylation by bacteria. *Environmental Science & Technology* **2014**, *48*, (5), 3007-3013.
505
- 506 13. Schaefer, J. K.; Rocks, S. S.; Zheng, W.; Liang, L. Y.; Gu, B. H.; Morel, F. M. M.,
507 Active transport, substrate specificity, and methylation of hg(ii) in anaerobic bacteria. *P Natl*
508 *Acad Sci USA* **2011**, *108*, (21), 8714-8719.
509
- 510 14. Schaefer, J. K.; Morel, F. M. M., High methylation rates of mercury bound to cysteine by
511 *Geobacter sulfurreducens*. *Nat Geosci* **2009**, *2*, (2), 123-126.
512
- 513 15. Lin, H.; Lu, X.; Liang, L. Y.; Gu, B. H., Cysteine inhibits mercury methylation by
514 *Geobacter sulfurreducens* pca mutant delta omcBestz. *Environ Sci Tech Let* **2015**, *2*, (5), 144-148.
515
- 516 16. Thomas, S. A.; Catty, P.; Hazemann, J.-L.; Michaud-Soret, I.; Gaillard, J.-F., The role of
517 cysteine and sulfide in the interplay between microbial hg(ii) uptake and sulfur metabolism.
518 *Metallomics* **2019**, *11*, (7), 1219-1229.
519
- 520 17. Thomas, S. A.; Rodby, K. E.; Roth, E. W.; Wu, J.; Gaillard, J.-F., Spectroscopic and
521 microscopic evidence of biomediated hgs species formation from hg(ii)-cysteine complexes:
522 Implications for hg(ii) bioavailability. *Environmental Science & Technology* **2018**, *52*, (17),
523 10030-10039.
524
- 525 18. Thomas, S. A.; Gaillard, J.-F., Cysteine addition promotes sulfide production and 4-fold
526 hg(ii)-s coordination in actively metabolizing *Escherichia coli*. *Environmental Science &*
527 *Technology* **2017**, *51*, (8), 4642-4651.
528
- 529 19. Graham, A. M.; Aiken, G. R.; Gilmour, C. C., Dissolved organic matter enhances
530 microbial mercury methylation under sulfidic conditions. *Environmental Science & Technology*
531 **2012**, *46*, (5), 2715-2723.
532
- 533 20. Adediran, G. A.; Liem-Nguyen, V.; Song, Y.; Schaefer, J. K.; Skyllberg, U.; Björn, E.,
534 Microbial biosynthesis of thiol compounds: Implications for speciation, cellular uptake, and
535 methylation of hg(ii). *Environmental Science & Technology* **2019**, *53*, (14), 8187-8196.
536

- 537 21. Thomas, S. A.; Tong, T. Z.; Gaillard, J. F., Hg(ii) bacterial biouptake: The role of
538 anthropogenic and biogenic ligands present in solution and spectroscopic evidence of ligand
539 exchange reactions at the cell surface. *Metallomics* **2014**, *6*, (12), 2213-2222.
540
- 541 22. Mishra, B.; Shoenfelt, E.; Yu, Q.; Yee, N.; Fein, J. B.; Myneni, S. C. B., Stoichiometry of
542 mercury-thiol complexes on bacterial cell envelopes. *Chem Geol* **2017**, *464*, 137-146.
543
- 544 23. Dunham-Cheatham, S.; Mishra, B.; Myneni, S.; Fein, J. B., The effect of natural organic
545 matter on the adsorption of mercury to bacterial cells. *Geochim Cosmochim Acta* **2015**, *150*, 1-10.
546
- 547 24. Dunham-Cheatham, S.; Farrell, B.; Mishra, B.; Myneni, S.; Fein, J. B., The effect of
548 chloride on the adsorption of hg onto three bacterial species. *Chem Geol* **2014**, *373*, 106-114.
549
- 550 25. Colombo, M. J.; Ha, J. Y.; Reinfelder, J. R.; Barkay, T.; Yee, N., Anaerobic oxidation of
551 hg(0) and methylmercury formation by *Desulfovibrio desulfuricans* nd132. *Geochim Cosmochim*
552 *Acta* **2013**, *112*, 166-177.
553
- 554 26. Manceau, A.; Bustamante, P.; Haouz, A.; Bourdineaud, J. P.; Gonzalez-Rey, M.;
555 Lemouchi, C.; Gautier-Luneau, I.; Geertsen, V.; Barriet, E.; Rovezzi, M.; Glatzel, P.; Pin, S.,
556 Frontispiece: Mercury(ii) binding to metallothionein in *Mytilus edulis* revealed by high energy-
557 resolution xanes spectroscopy. *Chemistry – A European Journal* **2019**, *25*, (4), 997-1009.
558
- 559 27. Bourdineaud, J.-P.; Gonzalez-Rey, M.; Rovezzi, M.; Glatzel, P.; Nagy, K. L.; Manceau,
560 A., Divalent mercury in dissolved organic matter is bioavailable to fish and accumulates as
561 dithiolate and tetrathiolate complexes. *Environmental Science & Technology* **2019**, *53*, (9), 4880-
562 4891.
563
- 564 28. Manceau, A.; Merkulova, M.; Murdzek, M.; Batanova, V.; Baran, R.; Glatzel, P.; Saikia,
565 B. K.; Paktunc, D.; Lefticariu, L., Chemical forms of mercury in pyrite: Implications for
566 predicting mercury releases in acid mine drainage settings. *Environmental Science & Technology*
567 **2018**, *52*, (18), 10286-10296.
568
- 569 29. Manceau, A.; Enescu, M.; Simionovici, A.; Lanson, M.; Gonzalez-Rey, M.; Rovezzi, M.;
570 Tucoulou, R.; Glatzel, P.; Nagy, K. L.; Bourdineaud, J. P., Chemical forms of mercury in human
571 hair reveal sources of exposure. *Environmental Science & Technology* **2016**, *50*, (19), 10721-
572 10729.
573
- 574 30. Manceau, A.; Lemouchi, C.; Enescu, M.; Gaillot, A. C.; Lanson, M.; Magnin, V.;
575 Glatzel, P.; Poulin, B. A.; Ryan, J. N.; Aiken, G. R.; Gautier-Luneau, I.; Nagy, K. L., Formation
576 of mercury sulfide from hg(ii)-thiolate complexes in natural organic matter. *Environmental*
577 *Science & Technology* **2015**, *49*, (16), 9787-9796.
578
- 579 31. Fein, J. B.; Yu, Q.; Nam, J.; Yee, N., Bacterial cell envelope and extracellular sulfhydryl
580 binding sites: Their roles in metal binding and bioavailability. *Chem Geol* **2019**, *521*, 28-38.
581

- 582 32. Mishra, B.; O'Loughlin, E. J.; Boyanov, M. I.; Kemner, K. M., Binding of hg-ii to high-
583 affinity sites on bacteria inhibits reduction to hg-0 by mixed fe-ii/iii phases. *Environmental*
584 *Science & Technology* **2011**, *45*, (22), 9597-9603.
585
- 586 33. Worms, I.; Simon, D. F.; Hassler, C. S.; Wilkinson, K. J., Bioavailability of trace metals
587 to aquatic microorganisms: Importance of chemical, biological and physical processes on
588 biouptake. *Biochimie* **2006**, *88*, (11), 1721-1731.
589
- 590 34. Joe-Wong, C.; Shoenfelt, E.; Hauser, E. J.; Crompton, N.; Myneni, S. C. B., Estimation
591 of reactive thiol concentrations in dissolved organic matter and bacterial cell membranes in
592 aquatic systems. *Environmental Science & Technology* **2012**, *46*, (18), 9854-9861.
593
- 594 35. Sholupov, S.; Pogarev, S.; Ryzhov, V.; Mashyanov, N.; Stroganov, A., Zeeman atomic
595 absorption spectrometer ra-915+ for direct determination of mercury in air and complex matrix
596 samples. *Fuel Processing Technology* **2004**, *85*, (6), 473-485.
597
- 598 36. Ravel, B.; Newville, M., Athena, artemis, hephaestus: Data analysis for x-ray absorption
599 spectroscopy using ifeffit. *J Synchrotron Radiat* **2005**, *12*, 537-541.
600
- 601 37. Newville, M., Larch: An analysis package for xafs and related spectroscopies. *J Phys*
602 *Conf Ser* **2013**, *430*.
603
- 604 38. Wang, Y. W.; Yu, Q.; Mishra, B.; Schaefer, J. K.; Fein, J. B.; Yee, N., Adsorption of
605 methylmercury onto geobacter bemidjensis bem. *Environmental Science & Technology* **2018**,
606 *52*, (20), 11564-11572.
607
- 608 39. Yu, Q.; Fein, J. B., Enhanced removal of dissolved hg(ii), cd(ii), and au(iii) from water
609 by bacillus subtilis bacterial biomass containing an elevated concentration of sulfhydryl sites.
610 *Environmental Science & Technology* **2017**, *51*, (24), 14360-14367.
611
- 612 40. Yu, Q.; Fein, J. B., Sulfhydryl binding sites within bacterial extracellular polymeric
613 substances. *Environmental Science & Technology* **2016**, *50*, (11), 5498-5505.
614
- 615 41. Yu, Q.; Szymanowski, J.; Myneni, S. C. B.; Fein, J. B., Characterization of sulfhydryl
616 sites within bacterial cell envelopes using selective site-blocking and potentiometric titrations.
617 *Chem Geol* **2014**, *373*, 50-58.
618
- 619 42. Hu, H. Y.; Lin, H.; Zheng, W.; Rao, B.; Feng, X. B.; Liang, L. Y.; Elias, D. A.; Gu, B.
620 H., Mercury reduction and cell-surface adsorption by geobacter sulfurreducens pca.
621 *Environmental Science & Technology* **2013**, *47*, (19), 10922-10930.
622
- 623 43. Proux, O.; Lahera, E.; Del Net, W.; Kieffer, I.; Rovezzi, M.; Testemale, D.; Irar, M.;
624 Thomas, S.; Aguilar-Tapia, A.; Bazarkina, E. F.; Prat, A.; Tella, M.; Auffan, M.; Rose, J.;
625 Hazemann, J.-L., High-energy resolution fluorescence detected x-ray absorption spectroscopy: A
626 powerful new structural tool in environmental biogeochemistry sciences. *Journal of*
627 *Environmental Quality* **2017**, *46*, (6), 1146-1157.

628
629 44. Manceau, A.; Lemouchi, C.; Rovezzi, M.; Lanson, M.; Gatzel, P.; Nagy, K. L.; Gautier-
630 Luneau, I.; Joly, Y.; Enescu, M., Structure, bonding, and stability of mercury complexes with
631 thiolate and thioether ligands from high-resolution xanes spectroscopy and first-principles
632 calculations. *Inorganic Chemistry* **2015**, *54*, (24), 11776-11791.
633
634 45. Masip, L.; Veeravalli, K.; Georgioui, G., The many faces of glutathione in bacteria.
635 *Antioxid Redox Sign* **2006**, *8*, (5-6), 753-762.
636
637 46. Slowey, A. J., Rate of formation and dissolution of mercury sulfide nanoparticles: The
638 dual role of natural organic matter. *Geochim Cosmochim Acta* **2010**, *74*, (16), 4693-4708.
639
640 47. Poulin, B. A.; Gerbig, C. A.; Kim, C. S.; Stegemeier, J. P.; Ryan, J. N.; Aiken, G. R.,
641 Effects of sulfide concentration and dissolved organic matter characteristics on the structure of
642 nanocolloidal metacinnabar. *Environmental Science & Technology* **2017**, *51*, (22), 13133-13142.
643
644 48. Enescu, M.; Nagy, K. L.; Manceau, A., Nucleation of mercury sulfide by dealkylation.
645 *Sci Rep-Uk* **2016**, *6*.
646
647 49. Enescu, M.; Manceau, A., High-level ab initio calculation of the stability of mercury-
648 thiolate complexes. *Theor Chem Acc* **2014**, *133*, (3).
649
650 50. Manceau, A.; Wang, J.; Rovezzi, M.; Glatzel, P.; Feng, X., Biogenesis of mercury-sulfur
651 nanoparticles in plant leaves from atmospheric gaseous mercury. *Environmental Science &*
652 *Technology* **2018**, *52*, (7), 3935-3948.
653
654 51. Wright, J. G.; Tsang, H. T.; Pennerhahn, J. E.; Ohalloran, T. V., Coordination chemistry
655 of the hg-merr metalloregulatory protein - evidence for a novel tridentate hg-cysteine receptor-
656 site. *J Am Chem Soc* **1990**, *112*, (6), 2434-2435.
657
658 52. Parks, J. M.; Smith, J. C., Chapter five - modeling mercury in proteins. In *Methods in*
659 *enzymology*, Voth, G. A., Ed. Academic Press: 2016; Vol. 578, pp 103-122.
660
661 53. Smith, S. D.; Bridou, R.; Johs, A.; Parks, J. M.; Elias, D. A.; Hurt, R. A.; Brown, S. D.;
662 Podar, M.; Wall, J. D., Site-directed mutagenesis of hgca and hgcb reveals amino acid residues
663 important for mercury methylation. *Applied and Environmental Microbiology* **2015**, *81*, (9),
664 3205-3217.
665
666 54. Zhou, J.; Riccardi, D.; Beste, A.; Smith, J. C.; Parks, J. M., Mercury methylation by hgca:
667 Theory supports carbanion transfer to hg(ii). *Inorganic Chemistry* **2014**, *53*, (2), 772-777.
668
669 55. Qian, C.; Johs, A.; Chen, H.; Mann, B. F.; Lu, X.; Abraham, P. E.; Hettich, R. L.; Gu, B.,
670 Global proteome response to deletion of genes related to mercury methylation and dissimilatory
671 metal reduction reveals changes in respiratory metabolism in geobacter sulfurreducens pca.
672 *Journal of Proteome Research* **2016**, *15*, (10), 3540-3549.
673

- 674 56. Date, S. S.; Parks, J. M.; Rush, K. W.; Wall, J. D.; Ragsdale, S. W.; Johs, A., Kinetics of
675 enzymatic mercury methylation at nanomolar concentrations catalyzed by hgca. *Applied and*
676 *Environmental Microbiology* **2019**, *85*, (13), e00438-19.
677
- 678 57. Goñi-Urriza, M.; Corsellis, Y.; Lancelour, L.; Tessier, E.; Gury, J.; Monperrus, M.;
679 Guyoneaud, R., Relationships between bacterial energetic metabolism, mercury methylation
680 potential, and hgca/hgcb gene expression in *desulfovibrio dechloroacetivorans* beroc1.
681 *Environmental Science and Pollution Research* **2015**, *22*, (18), 13764-13771.
682
- 683 58. Liu, Y. R.; Lu, X.; Zhao, L. D.; An, J.; He, J. Z.; Pierce, E. M.; Johs, A.; Gu, B. H.,
684 Effects of cellular sorption on mercury bioavailability and methylmercury production by
685 *desulfovibrio desulfuricans* nd132. *Environmental Science & Technology* **2016**, *50*, (24), 13335-
686 13341.
687
- 688 59. Zhao, L.; Li, Y.; Zhang, L.; Zheng, J.; Pierce, E. M.; Gu, B., Mercury adsorption on
689 minerals and its effect on microbial methylation. *ACS Earth and Space Chemistry* **2019**.
690
- 691 60. Graham, A. M.; Bullock, A. L.; Maizel, A. C.; Elias, D. A.; Gilmour, C. C., Detailed
692 assessment of the kinetics of hg-cell association, hg methylation, and methylmercury degradation
693 in several *desulfovibrio* species. *Applied and Environmental Microbiology* **2012**, *78*, (20), 7337-
694 7346.
695
696
697
698
699 **TOC**
700

